Electronic Supplementary Material (ESI) for Inorganic Chemistry Frontiers.

Supporting information

Self-assembly of tetra-nuclear lanthanide clusters via atmospheric CO_2 fixation: interesting solvent-induced structures and magnetic relaxation conversions

Wen-Min Wang[a,c], Zhi-Lei Wu[a,c*], Ya-Xin Zhang[a], Hai-Ying Wei[a], Hong-Ling Gao[b], Jian-Zhong Cui[b*]

[a] *College of Chemistry and Environmental Science, Hebei University, Baoding, 071002, P. R. China.*

[b] *Department of Chemistry, Tianjin University, Tianjin, 300354, China.*

[c] *Key Laboratory of Advanced Energy Materials Chemistry (Ministry of Education), Nankai University, Tianjin 300071, PR China.*

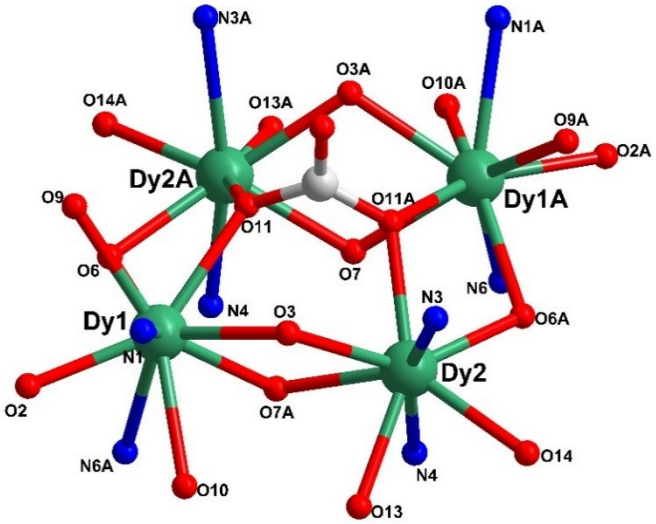

Fig. S1 Perspective view of the Dy_4 clusters in compound **2**.

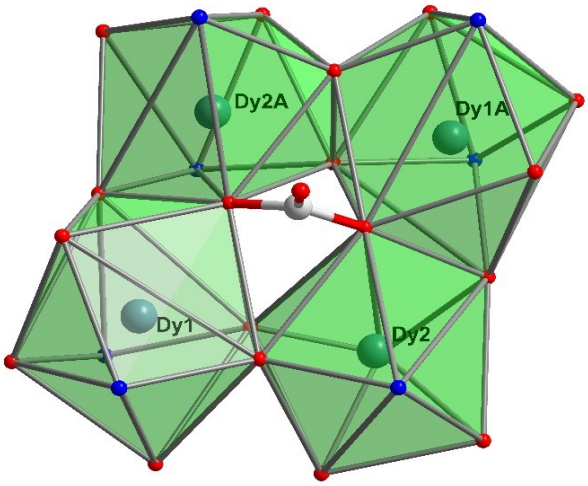

Fig. S2 The coordination polyhedrons of Dy(III) ions observed in **2**.

*Corresponding author. E-mail: cuijianzhong@tju.edu.cn.
*Corresponding author. E-mail: wuzhilei03@163.com.

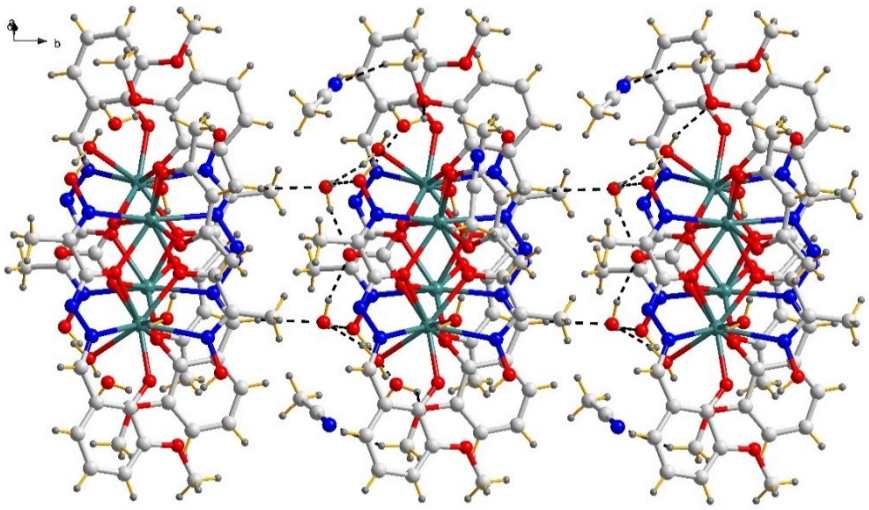

Fig. S3 The 3D packing diagram of **2** along the *c* axis.

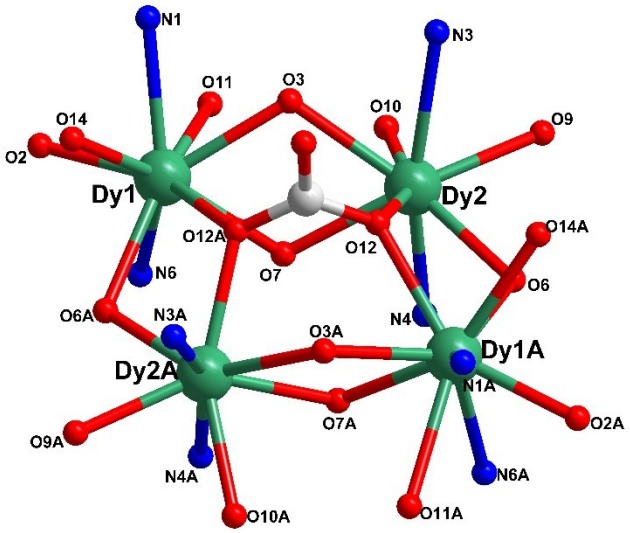

Fig. S4 Perspective view of the Dy_4 clusters in compound **4**.

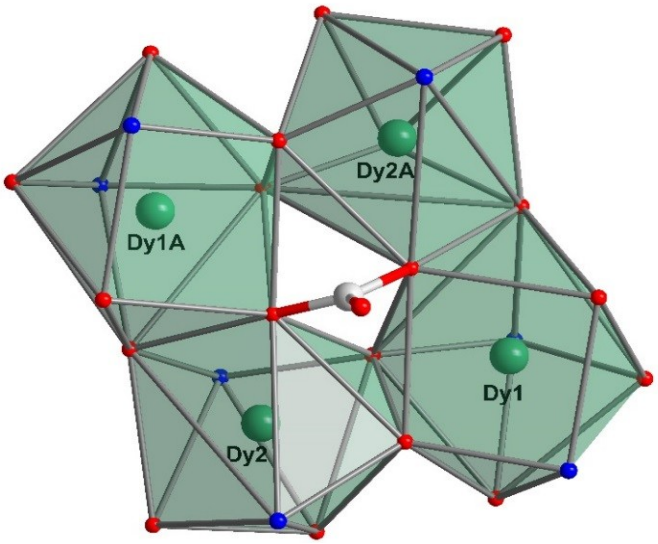

Fig. S5 The coordination polyhedrons of Dy(III) ions observed in **4**.

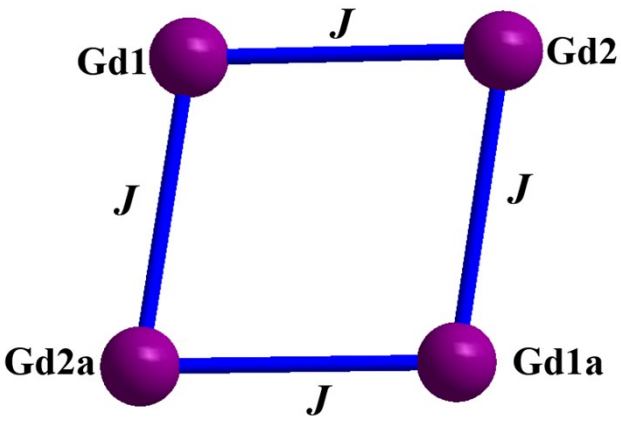

Fig. S6 The model used to fit the $\chi_M T$~T plots for **1** and **3**.

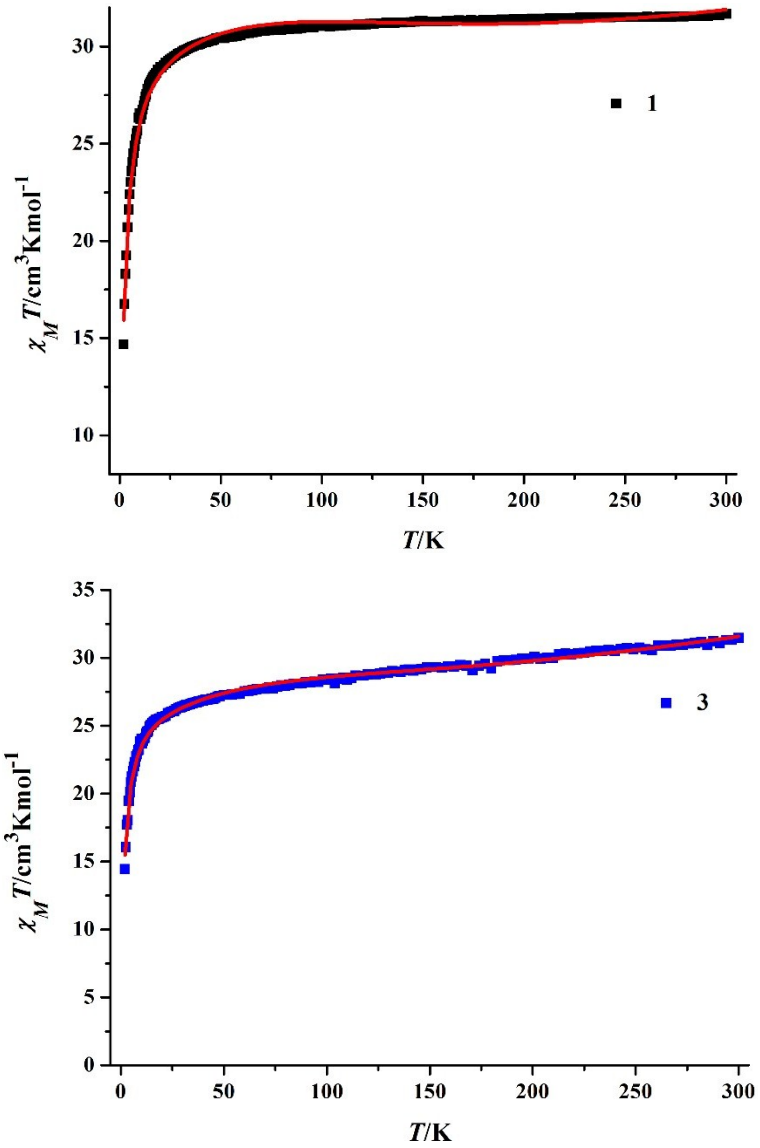

Fig. S7 The $\chi_M T$~T plots for **1** and **3** in the range of 2-300 K. The solid red lines are the best fit obtained.

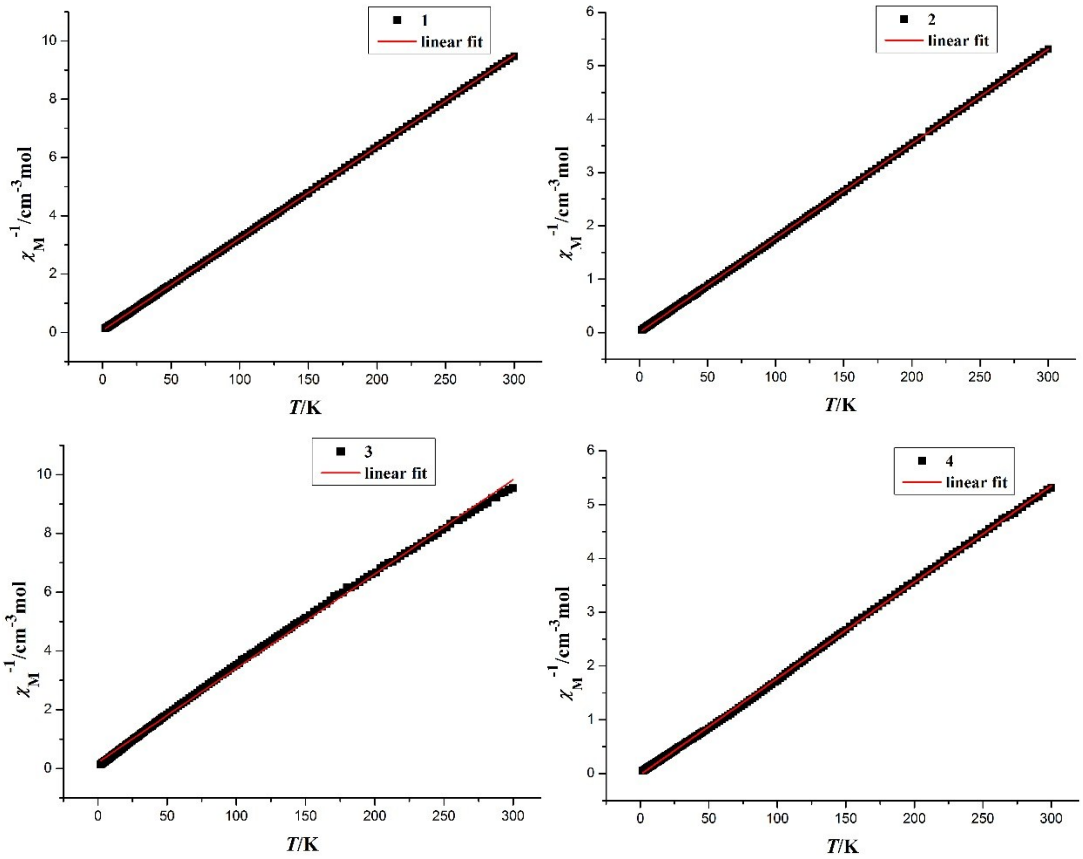

Fig. S8 The χ_M^{-1} versus T and the Curie-Weiss linear fit for **1**-**4**.

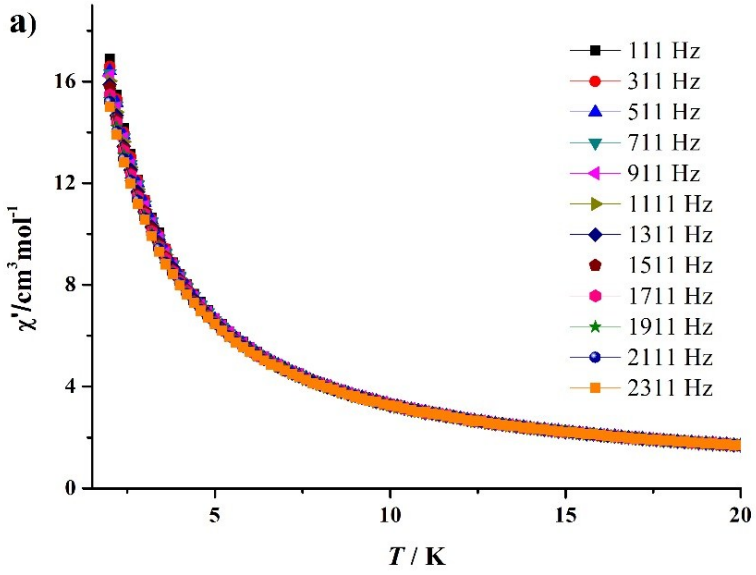

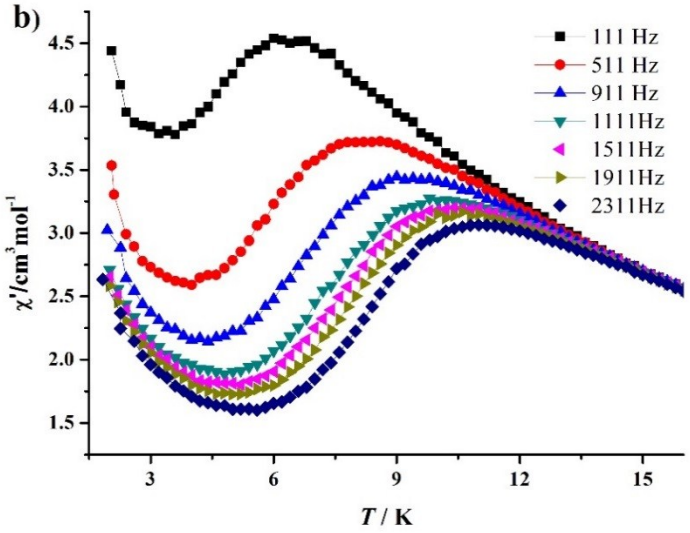

Fig. S9 Temperature-dependent of in-phase (χ') ac susceptibilities of compounds **2** (a) and **4** (b) under zero dc field.

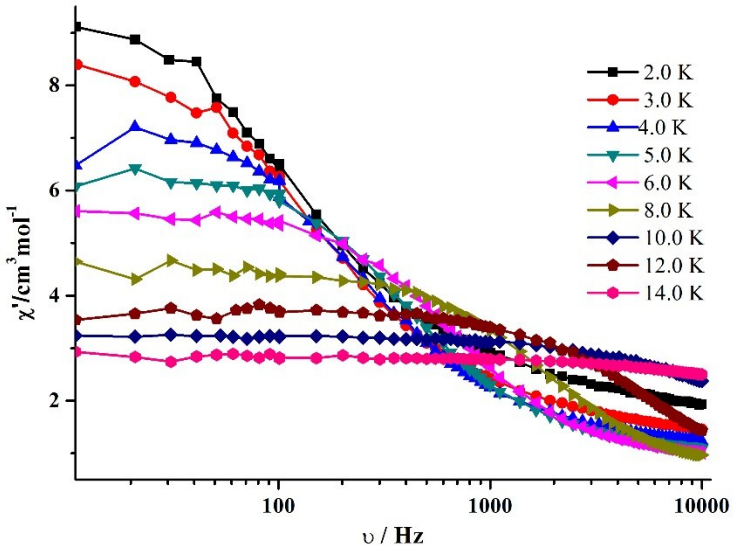

Fig. S10 Frequency-dependence of in-phase (χ') ac susceptibility for compound **4**.

Table S1 Crystallographic Data and Structure Refinements for compounds **1-4**.

	1	**2**	**3**	**4**
Formula	$C_{63}H_{86}Gd_4N_{16}O_{31}$	$C_{63}H_{86}Dy_4N_{16}O_{31}$	$C_{59}H_{82}Gd_4N_{12}O_{31}$	$C_{59}H_{82}Dy_4N_{12}O_{31}$
Fw	2192.47	2213.47	2084.36	2041.28
T/K	150(0)	150(0)	150(0)	150(0)
Cryst syst	Monoclinic	Monoclinic	Trigonal	Trigonal
Space group	*C*2/*c*	*C*2/*c*	$P3_121$	$P3_121$
a/Å	38.215(3)	38.452(4)	14.5700(3)	14.5121(3)
b/Å	10.6514(8)	10.5678(1)	14.5700(3)	14.5121(3)
c/Å^3	22.7866(2)	22.653(2)	36.0887(14)	36.4462(12)
α/°	90	90	90	90
β/°	122.547(2)	122.572(3)	90	90
γ/°	90	90	120	120
Volume/Å	7818.5(11)	7757.4(12)	6634.7(4)	6647.3(4)
Z	4	4	3	3
ρ_{calc}mg/mm^3	1.863	1.895	1.565	1.530
μ/mm^{-1}	3.443	3.903	3.037	3.406
F(000)	4320	4352	3072	2988
θ/°	2.263 to 25.009	2.258 to 26.448	2.339 to 26.424	3.231 to 25.005
Reflections collected	43932	49235	70862	23048
Unique reflns	6821 [R_{int}=0.0573]	7941 [R_{int}=0.0301]	9076 [R_{int}=0.0466]	7744 [R_{int} = 0.0467]
GOF on F^2	1.039	1.057	1.065	1.040
R_1, wR_2 ($I > 2\sigma(I)$)	0.0469, 0.1145	0.0237, 0.0561	0.0398, 0.1169	0.0406, 0.0887
R_1, wR_2 (all data)	0.0611, 0.1268	0.0289, 0.0582	0.0447, 0.1191	0.0475, 0.0924

Table S2 The Dy(III) geometry analysis by SHAPE 2.0 for complexes **2** and **4**.

$Dy1^{III}$	C_{4v}JCSAPR	C_{4v}CSAPR	D_{3h}JTCTPR	D_{3h}TCTPR	C_sMFF
Cluster **2**	1.569	0.727	3.174	1.727	1.201
Cluster **4**	1.505	0.706	2.905	1.652	1.137
$Dy2^{III}$	D_{4d}SAPR	D_{2d}TDD	C_{2v}JBTPR	C_{2v}BTPR	D_{2d}JSD
Cluster **2**	3.476	2.698	3.973	3.086	6.117
Cluster **4**	4.519	2.822	4.582	3.636	6.360

Table S3. Comparison of the $-\Delta S_m^{max}$ values of **1** and **3**.

Compounds	M_w/N_{Gd}	Magnetic interaction [θ, K]	$-\Delta S_m^{max}$ [J kg^{-1}K^{-1}]
1	548.1	-1.23	31.23
3	521.1	-6.31	27.06

Table S4. The main structural parameters in complexes **2** and **4**.

Average distances		Compounds **2**	Compounds **4**
d(Dy---L^{2-}-O)	(Å)	2.3499	2.3371
d(Dy---acac-O)	(Å)	2.3443	2.3218
d(Dy---carbonate-O)	(Å)	2.3947	2.3887
d(Dy---solvents-O)	(Å)	2.5232	2.5164
d(Dy---N)	(Å)	2.5213	2.5188
d(Dy---Dy)	(Å)	3.9020	3.8924